

# AUTOMATED MODE RECOGNITION ALGORITHM FOR ACCELERATING CAVITIES\*

K. Brackebusch<sup>†</sup>, T. Galek, U. van Rienen, Institute of General Electrical Engineering, University of Rostock, Germany

## Abstract

Eigenmode simulations of accelerating structures often involve a large number of computed modes that need to be cataloged and compared. In order to effectively process all the information gathered from eigenmode simulations a new algorithm was developed to automatically recognize modes' field patterns. In this paper we present the principles of the algorithm and investigate its applicability by means of different single and multicell cavities. The highest achievable order of correctly recognized modes is of particular interest.

## INTRODUCTION

The simplest way to order eigenmodes of an accelerating cavity is to sort them by increasing resonant frequency, starting with the fundamental mode. Additionally, the modes can be classified by their electromagnetic field, regarding vanishing or non-vanishing field components and the distribution of local extrema inside the cavity. This classification is needed for recognition of the accelerating mode, differentiation of higher order modes (monopole, dipole, quadrupole, etc.) and separation into passbands. It provides basic information for analyzing the performance characteristics of the cavity. For instance, solely monopole modes have a longitudinal field component on the beam axis, thus their interaction with the particle beam is inherently different from other modes.

The manual recognition of a mode is time consuming especially if a particular mode has to be detected amongst a group of modes. Therefore an automated mode recognition algorithm may be a useful additional tool for designing accelerating cavities.

## THEORY

The eigenmodes of a cylindrical pillbox cavity can be differentiated into transversal magnetic (TM) and transversal electric (TE) modes depending on whether the electric or magnetic field vanishes in longitudinal direction. Further, they can be identified by an azimuthal ( $m$ ), a radial ( $n$ ) and a longitudinal index ( $p$ ) that are deduced from the number of local field extrema (or zero crossings) in the respective direction. So, each pillbox mode can be designated as  $TM_{mnp}$  or  $TE_{mnp}$ . The azimuthal index also determines the mode designation as a monopole ( $m=0$ ), dipole ( $m=1$ ), etc. Except for monopole modes all modes exist in two polarizations differentiable by a polarization angle. (In the following, the mode polarization is neglected.)

\* Work supported by Federal Ministry for Research and Education (BMBF) under contract 05K13HR1

<sup>†</sup> korinna.brackebusch@uni-rostock.de

By continuous deformation, a pillbox shape can be transformed into any other (simply connected) cavity shape. Thereby, frequencies and fields of the modes change but each mode of the deformed cavity still matches a particular mode of the pillbox cavity. Accordingly, the same nomenclature as for a pillbox cavity could be used. But in practice, this only makes sense to a certain extent. With increasing frequency the differentiation into TM and TE modes becomes less and less reasonable since neither the electric ( $E_z$ ) nor the magnetic longitudinal field ( $H_z$ ) completely vanishes due to the deformed boundary. Only a small number of modes, primarily modes with a low frequency, can be identified as TM or TE. Modes with both components,  $E_z$  and  $H_z$ , (or at least without a clearly dominant longitudinal field) are designated as hybrid modes.

Combining multiple single cell cavities to one multicell cavity creates a system of coupled oscillators. The coupling between the modes of the single cells leads to passbands of modes. This means that inside a multicell cavity consisting of  $N$  cells with similar shape for each single cell mode  $N$  equivalent modes exist. The smaller the cell-to-cell coupling, the smaller is the frequency shift between the passband modes and the more similar are the field patterns in the cells. The maximal field amplitude differs in each cell  $i$  and for each passband mode  $b$  ( $i, b \leq N$ ). For cavities tuned to field flatness the amplitude is nearly proportional to a sinusoidal function [1]

$$Ampl. \propto \sin(b\pi \frac{2i-1}{2N}). \quad (1)$$

So, a multicell mode can additionally be denominated by its phase advance as  $b\pi/N$  mode (see fig. 1).

It is now of particular interest to which extent the pillbox nomenclature can be applied to modes of accelerating cavities. Accelerating cavities usually are cylindrically symmetric structures. The fields inside these structures show a sinusoidal behavior in azimuthal direction, like pillbox modes. Hence, the azimuthal index  $m$  stays the same. However, this is not the case for the radial and longitudinal indices.

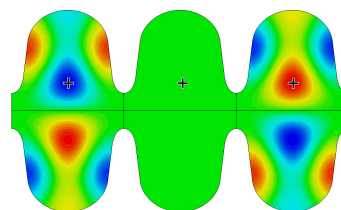


Figure 1: Azimuthal magnetic field  $H_\varphi$  of  $TM_{012} 2\pi/3$ . The coordinates for recognition of passband index  $b$  are marked.

Content from this work may be used under the terms of the CC BY 3.0 licence (© 2014). Any distribution of this work must maintain attribution to the author(s), title of the work, publisher, and DOI.

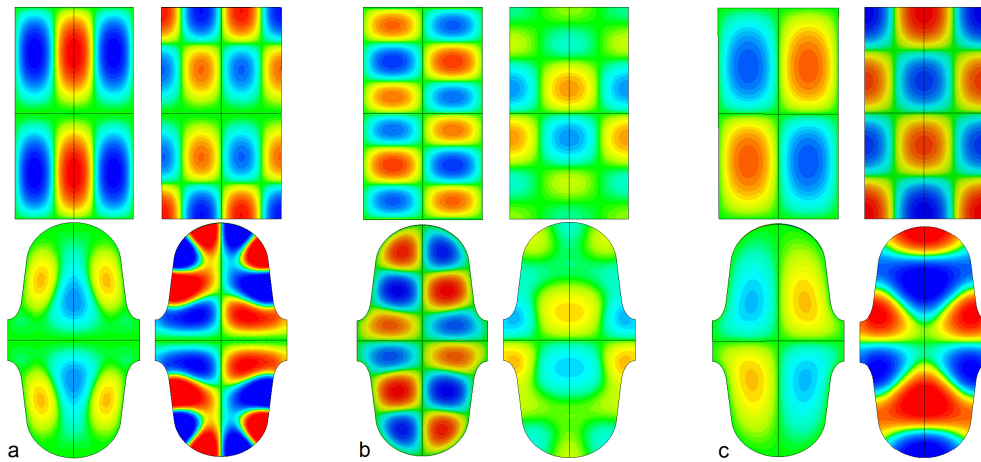


Figure 2: Fields of  $TM_{313}$  (a),  $TE_{232}$  (b) and  $TM_{212}$  (c) mode inside a pillbox cavity (top) and corresponding mode inside an elliptical cavity (bottom). Each sub-figure shows the azimuthal fields  $E_\varphi$  (left) and  $H_\varphi$  (right) in the longitudinal cut plane. The amplitudes are scaled logarithmically.

Due to the boundary deformation the distribution of local extrema in the longitudinal cut plane changes. The extrema or more precisely the areas with same sign are shifted. Furthermore, such an area may split or multiple areas may unite to one. Fig. 2 illustrates this by means of an elliptical cavity. Observing several pillbox modes and their corresponding modes inside an elliptical cavity indicated a certain regularity in the transformation of the field patterns. This implies that although it may not be possible to recognize the radial and longitudinal indices  $n$  and  $p$  but that there may be found some equivalent indices that clearly differentiate the modes.

### ALGORITHM

The mode recognition algorithm is implemented in CST Microwave Studio [2] using a Visual Basic Macro. To decide if a mode is TM, TE or hybrid it must be determined if the longitudinal electric or magnetic field vanishes inside the cavity. Proving that  $E_z$  or  $H_z$  is zero inside the entire cavity is expensive and influenced by numerical errors. Therefore, the algorithm instead detects if  $E_z$  or  $H_z$  is dominant by comparing their maximal absolute amplitude  $E_{zMax}$  and  $H_{zMax}$ . This is done by applying a coarse Cartesian grid to the cavity volume (or the positive coordinate range if the shape has symmetries) and sampling  $E_z$  and  $H_z$  in the grid points. A mode is recognized as TM if

$$\frac{E_{zMax}}{H_{zMax}} > a \sqrt{\frac{\mu_0}{\epsilon_0}} \quad (2)$$

and as TE if

$$\frac{E_{zMax}}{H_{zMax}} < \frac{1}{a} \sqrt{\frac{\mu_0}{\epsilon_0}} \quad (3)$$

So the ratio of  $E_{zMax}$  and  $H_{zMax}$  is compared to free space impedance. An additional multiplier  $a$  is introduced to guarantee a reliable distinction of TM and TE by scaling the comparison value by a selectable order of magnitude. As mentioned in the previous section, in any case both  $E_z$  and

$H_z$  are non-zero at the boundary if it is not perpendicular to  $z$ . To prevent this effect,  $E_z$  and  $H_z$  are not sampled inside the entire cavity but inside a reduced volume omitting the boundary region (see fig. 3a).

Because of this boundary effect the longitudinal field is also not the most appropriate to recognize the mode indices. The azimuthal field components  $E_\varphi$  (instead of  $H_z$ ) and  $H_\varphi$  (instead of  $E_z$ ) are more suitable since the azimuthal direction is always tangential to the boundary of a cylindrically symmetric shape. Of course, the number and distribution of extrema differs for longitudinal and azimuthal fields but the relation is linear and the indices are only shifted by a constant offset. So, introducing these new mode indices is reasonable. Each index is defined as the number of local field extrema in the respective direction. Since both  $E_\varphi$  and  $H_\varphi$  have non-zero amplitudes also the indices of both fields ( $m_e, n_e, p_e$  and  $m_h, n_h, p_h$ ) are recognized. This provides maximal information about the field pattern.  $m_e, n_e$  and  $p_e$  are determined by firstly sampling  $E_\varphi$  on the coarse grid to detect the position  $r_{e\varphi}$  of maximal absolute amplitude  $E_{\varphi Max}$ . Then,  $E_\varphi$  is precisely sampled along three curves in radial, azimuthal and longitudinal direction through  $r_{e\varphi}$  as shown in fig. 3b. At this, a threshold for non-zero values (relative to  $E_{\varphi Max}$ ) is defined to avoid wrong indices due to

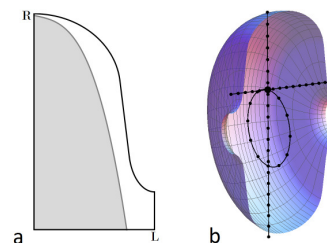


Figure 3: a) Elliptical cell shape and reduced shape (described by a simple polynomial). b) Discrete field points along curves in radial, azimuthal and longitudinal direction that cross the coordinates of maximal amplitude.

fluctuations around zero. Finally  $m_e$ ,  $n_e$  and  $p_e$  are deduced from the number of sign changes along the respective curve ( $0 \leq \varphi \leq \pi$ ,  $-R \leq r \leq R$  and  $0 \leq z \leq L$ ).  $m_h$ ,  $n_h$  and  $p_h$  are obtained from  $H_\varphi$  using the same procedure.

For investigating multicell structures the algorithm contains some extended features. Firstly, after detecting the positions of maximal field amplitude ( $\mathbf{r}_{e\varphi}$ ,  $\mathbf{r}_{h\varphi}$ ), the sampling range for  $p_e$  and  $p_h$  is reduced to that cell where  $\mathbf{r}_{e\varphi}$  and  $\mathbf{r}_{h\varphi}$  are located. Secondly, the passband index  $b$  is identified using eq. (1) and sampling the dominant azimuthal field, either  $E_\varphi$  or  $H_\varphi$ , in longitudinal direction. The field is only sampled once per cell, starting in  $\mathbf{r}_{e\varphi}$  and  $\mathbf{r}_{h\varphi}$  respectively, and shifting the position by exactly one cell length through the entire structure (see fig. 1).

## RESULTS

The algorithm was successfully applied to pillbox modes ( $R = 102.88$  mm,  $L = 115.38$  mm) from 1.15 GHz up to 10 GHz. All mode types (TM or TE) and mode indices  $m_e$ ,  $n_e$ ,  $p_e$ ,  $m_h$ ,  $n_h$ ,  $p_h$  were correctly recognized. Mode types and indices were also examined for an elliptical single cell (same  $R$ ,  $L$ ) by comparing more than 100 modes from 1.24 GHz up to 7.35 GHz with their corresponding pillbox modes. Table 1 provides a selection of these modes. The azimuthal indices  $m_e$  and  $m_h$  were always correctly detected, so a differentiation into monopole modes, dipole modes, etc. is in any case possible. The recognition of TM and TE modes, if identified, was also errorless. At this, it turned out that TM modes could be recognized over a larger frequency range than TE modes. Of course, not all elliptical cavity modes has the same indices as their equivalent pillbox modes. Differences in the indices arise from the shifting of the extrema distribution as comparing the indices of table 1 with fig. 2 illustrates. For instance, the areas with same sign of  $\text{TM}_{mnp}$  modes with even  $p$  are shifted into "longitudinal belts" leading to decreased  $p_e$ ,  $p_h$  and/or increased  $n_e$ ,  $n_h$  (see fig. 2c). Most important is that no combination of mode indices occurred twice for the elliptical cell. Consequently, an individual mode nomenclature is achievable making it possible to differentiate the modes according to regularities of their mode indices.

The algorithm was also successfully applied to multicell cavities. Modes from 1.24 GHz up to 5.90 GHz were examined for an elliptical 3-cell cavity and all of them were correctly recognized. This means that there were always three passband modes of same type and identical mode indices but different passband indexes  $b$  (1 to 3) on condition that the modes coupled between the cells. Passband modes that do not couple to neighboring cells are independent from another and therefore also had repetitive values for  $b$ . To test to which extent the algorithm can handle the effects of strong cell-to-cell coupling additionally a 5-cell cavity with large iris radius was investigated. Since the field pattern can substantially vary from cell to cell due to a high coupling this is of particular interest. Between 1.27 GHz and 4.58 GHz two passbands with a wrong indexed mode were found. The wrong index is in fact caused by a coupling-based shift of

05 Beam Dynamics and Electromagnetic Fields

D06 Code Developments and Simulation Techniques

Table 1: Mode Indices of Pillbox Cavity Modes and Corresponding Elliptical Cavity Modes. The last Column Additionally Shows the Dominant Azimuthal Field

mode	Pillbox cavity						Elliptical cavity						dom.	
	$m_e$	$n_e$	$p_e$	$m_h$	$n_h$	$p_h$	type	$m_e$	$n_e$	$p_e$	$m_h$	$n_h$		$p_h$
TM <sub>010</sub>	-	-	-	0	2	1	TM	-	-	-	0	2	1	$H_\varphi$
TE <sub>111</sub>	1	1	1	1	1	2	hy	1	1	1	1	1	2	$E_\varphi$
TE <sub>311</sub>	3	1	1	3	1	2	TE	3	1	1	3	1	2	$E_\varphi$
TM <sub>212</sub>	2	2	2	2	4	3	TM	2	2	2	2	6	1	$H_\varphi$
TM <sub>113</sub>	1	1	3	1	3	4	TM	1	1	3	1	5	2	$H_\varphi$
TE <sub>612</sub>	6	2	2	6	2	3	hy	6	2	2	6	2	3	$H_\varphi$
TM <sub>321</sub>	3	3	1	3	5	2	TM	3	3	1	3	5	2	$H_\varphi$
TM <sub>313</sub>	3	1	3	3	3	4	TM	3	1	3	3	5	2	$H_\varphi$
TE <sub>422</sub>	4	4	2	4	4	3	hy	4	4	2	4	4	3	$E_\varphi$
TE <sub>232</sub>	2	6	2	2	6	3	TE	2	6	2	2	4	3	$E_\varphi$
TE <sub>214</sub>	2	2	4	2	2	5	hy	2	2	4	2	4	5	$H_\varphi$
TM <sub>230</sub>	-	-	-	2	8	1	TM	2	4	2	2	8	3	$H_\varphi$
TM <sub>422</sub>	4	4	2	4	6	3	TM	4	4	2	4	6	1	$H_\varphi$
TE <sub>622</sub>	6	4	2	6	4	3	hy	6	4	2	6	4	3	$E_\varphi$
TM <sub>042</sub>	-	-	-	0	8	3	TM	-	-	-	0	8	1	$H_\varphi$
TM <sub>812</sub>	8	2	2	8	4	3	TM	8	2	2	8	6	1	$H_\varphi$
TM <sub>414</sub>	4	2	4	4	4	5	TM	4	6	2	4	8	3	$H_\varphi$

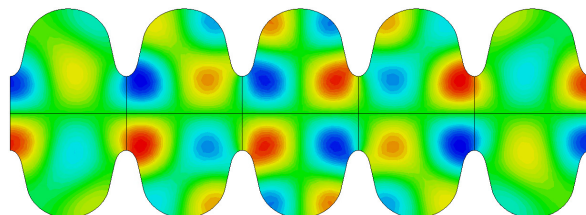


Figure 4:  $H_\varphi$  of a  $\text{TM}_0$  mode at 3.57 GHz: Due to a shift of its field pattern the longitudinal index  $p_h$  is 2 for the middle cell and 3 for the rest of the cells.

the field pattern beyond the single cell boundaries as fig. 4 illustrates. But since the other four modes in the passband have identical indices the wrong index can be easily detected. Above 4.59 GHz it gets more and more difficult to find completely matching sets of passband modes. The field patterns may increasingly shift, so, eq. (1) is no longer valid. Hence, a strong cell-to-cell coupling combined with a large number of cells reduces the order of fully correct recognized modes. However, a correct detection of mode type and azimuthal index is guaranteed even for very high frequencies.

In conclusion, an automated mode recognition algorithm was introduced feasible to classify cylindrically symmetric single and multicell cavities of arbitrary shape that allows for an individual nomenclature for numerous modes.

## REFERENCES

- [1] H. Padamsee, J. Knobloch, T. Hays, *RF Superconductivity for Accelerators*, Wiley VCH, 2nd Edition, 2008.
- [2] Computer Simulation Technology AG, *Microwave Studio®*, 64289 Darmstadt, Germany.